Comparative Study on Optimization Methods for a Motor-Drive of Artificial Hearts

André Pohlmann, Marc Leßmann and Kay Hameyer
Institute of Electrical Machines, RWTH Aachen University, Germany
E-mail: Andre.Pohlmann@iem.rwth-aachen.de

Abstract — Worldwide cardiovascular diseases are the major cause of death. Beside heart transplants, which is a limited option due to the available number of human donor hearts, artificial hearts are the only therapy available for terminal heart diseases. For various reasons a total implantable artificial heart is desirable. But the limited space in the human thorax sets rigorous restrictions regarding the weight and the dimensions of the device. Nevertheless the appropriate functionality of the artificial heart must be ensured and blood damage must be prevented. These requirements set further restrictions to the drive of this device. In this paper two optimization methods, which are manual parameter variation and Differential Evolution (DE) algorithm, are presented, to match the specifications of an artificial heart.

I. INTRODUCTION

For the therapy of heart diseases artificial hearts are required, because heart transplants are only a limited option. Currently, there is only one clinical approved total artificial heart systems worldwide, which is the Cardio West [1]. In order to avoid its connections through the human abdominal wall, it is desirable to completely implant an artificial heart into the human thorax. This will improve the quality of life of the patient and reduces the risk of infections. Considering the available limited space in the human thorax, it is obvious that the weight and dimensions of an implantable artificial heart and its drive are restricted. Nevertheless the drive has to provide the required force for the blood pump to achieve a sufficient perfusion of the human body. The resulting losses of the blood pump must be limited to avoid blood damage by overheating.

Fig. 1a presents the drive`s bisection of a pulsatile artificial heart, developed at the Institute of Electrical Machines of the RWTH Aachen University [2], which optimization subjects to two objectives is studied here. The drive is excited by an inner and an outer permanent magnet ring, made of Neodymium Iron Bor (NdFeB). Compared to the remanent induction $B_{r,in}$ of the inner magnet ring, which amounts to 1.44 T, the remanent induction $B_{r,out}$ of the outer magnet ring only averages to 1.35 T. Above and beyond the magnets, pole shoes are attached, concentrating the induction in the air gap. They are made of an iron vanadium cobalt alloy, referred here by its commercial name Vacoflux, which has a saturation induction of 2.4 T [3]. The mover consists of four coils. Each coil is hand wounded with a rectangular copper wire. By this way a copper fill factor of 75 % is achieved. In Fig. 1b the magnetization of the magnets and the flux path is indicated by arrows. When supplying the coils with a dc current, the moving direction of the coils can be obtained by applying the Lorentz force equation (1). The weight of the drive amounts to 616 g. During simulation the electric losses occurring in the drive were determined to 8 W [4], while providing the required forces, given in Fig. 2, for allowing the blood pump a sufficient perfusion of the human body. As the medium aortic pressure of 100 mmHg is much higher than in the pulmonary blood circuit, which amounts to 27 mmHg, the absolute value of the required forces for pumping the blood in the left blood circuit are much higher when compared to the required forces provided for the right blood circuit.

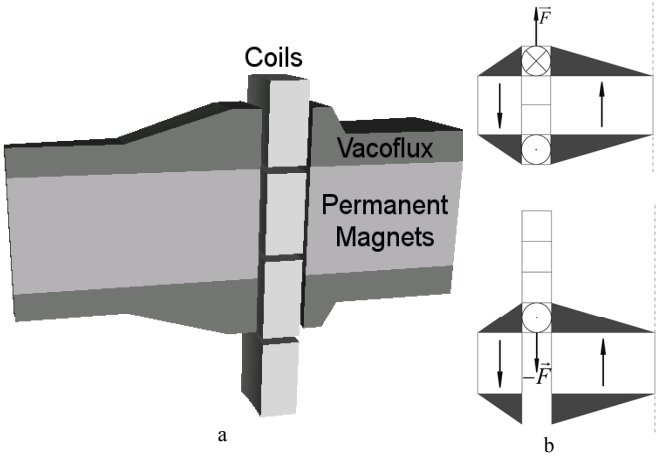

Fig. 1 Drive of an artificial heart.

II. OPTIMIZATION CHAIN

Both optimization methods, introduced in the next section, are working with the following optimization chain, which consists of three steps. Based on the input parameters a mesh is generated. This mesh is required for the following FEM simulation of the induction distribution in the air gap of the drive. During the last step the weight and the losses of the modeled drive is analytically calculated. In order to achieve a good efficiency an optimal current supply of the coils in dependency of the air gap induction is determined, based on the required forces.

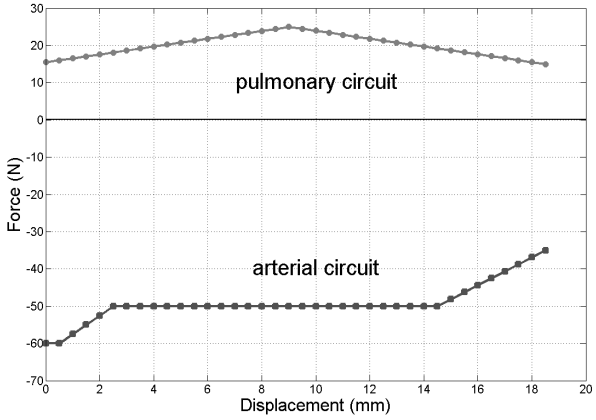

Fig. 2 Force vs. Displacement characteristic for the optimization.

A. parameter input

In order to automate the optimization process a parameterizable computer model is establish for the mesh generation, required for the following FEM simulations. As it is presented in Fig. 3 the model is defined by five fixed parameters (a - e) and seven variable parameters. For the generation of the computer model and the mesh, a parameter file is created, which initializes the variables.

B. FEM simulation

According to the Lorentz force equation

$$\vec{F}_n(x) = I_n(x) \cdot (\vec{l} \times \vec{B}_n(x)) \quad (1)$$

the radial magnetic field distribution $\overline{B}_{r,n}(x)$ in the air gap is required to determine the force output. As the magnetic leakage flux is significant and the iron vanadium cobalt alloy is magnetically saturated, Fig. 4, non linear FEM simulations, performed by a 3d static problem solver from the Institute of Electrical Machines in-house FE-software package iMoose[5], are applied here in order to obtain the induction.

C. Calculation of weight and losses

For the optimization the weight and the resulting losses have to be computed. While the total weight of the drive can be calculated by multiplying the volumes, extracted from CAD models, with their material densities and accumulating the resulting weights, a calculation chain is required to determine the resulting losses. Due the air gap width of about 4 mm between the inner and outer permanent magnet ring, the counter effects of the field, excited by the coils, can be neglected. Additionally, iron losses in the pole shoes and in the permanent magnets are negligible in the operation frequency range between 1.33 and 2.66 Hz. Hence, the ohmic losses for each coil are dominating. In order to keep the losses as low as possible the coils should be supplied depending on the average radial magnetic field distribution $\overline{B}_{r,n}(x)$ in the air gap, penetrating each coil n at displacement x. Therefore, so called current factors $k_{I,n}(x)$ are calculated by evaluating the induction distribution, obtained by the previous FEM simulations, for each coil and each position x of the axial displacement

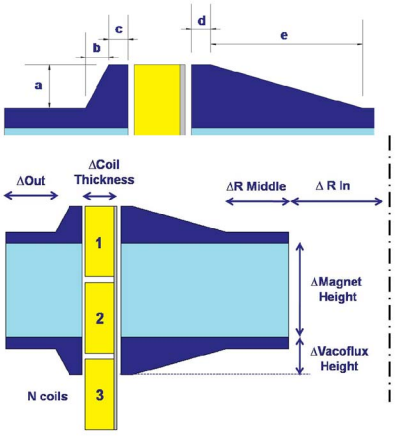

Fig. 3 Parameterized drive for optimization.

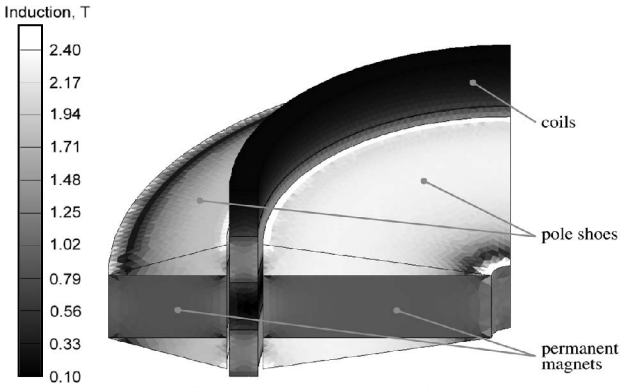

Fig. 4 Distribution of the induction in the drive.

$$k_{I,n}(x) = \frac{\overline{B}_{r,n}(x)}{\sum_{n=1}^{4} \left|\overline{B}_{r,n}(x)\right|}. \quad (2)$$

Before the current supply $I_{n,fw/bw}(x)$ for each coil can be calculated by

$$I_{n,fw/bw}(x) = k_{I,n}(x) \cdot I_{sum,fw,bw}(x), \quad (3)$$

the current value $I_{sum,fw,bw}(x)$ has to be determined. Therefore the Lorentz force equation (1) is transformed to

$$I_{sum,fw/bw}(x) = \frac{F_{required,fw/bw}(x)}{\sum_{n=1}^{4} \overline{B}_{r,n}(x) \cdot k_{I,n}(x) \cdot l}. \quad (4)$$

The force $F_{required,fw/bw}(x)$, which has to be provided for the blood pump, can be obtained from Fig. 2 . As the forces, required for pumping the blood, differ for the pulmonary and the arterial blood circuit, the annotations fw (pulmonary) and bw (arterial) indicate the moving direction of the coils. Finally, the resulting ohmic losses $P_{sum,fw/bw}(x)$ are determined by accumulating the ohmic losses of each coil, which are calculated by multiplying the square of the coil's current $I_{n,fw/bw}(x)$ with the winding resistance R:

$$P_{sum,fw/bw}(x) = \sum_{n=1}^{4} I^2_{n,fw/bw}(x) \cdot R. \quad (5)$$

In order to compute the average losses during one beat cycle, the maximum axial displacement of the pusher plates of 18.5 mm is divided into segments with a length of 0.5 mm:

$$x_m = m \cdot 0.5mm, \quad m = 0,...37. \quad (6)$$

For each of these m segments the delay time t_m of the pusher plates within each segment is calculated, based on the assumption of a sinusoidal movement of the pusher plates:

$$t_m = \frac{\arcsin\left(\frac{x_{m+1} - 9.25mm}{9.25mm}\right) - \arcsin\left(\frac{x_m - 9.25mm}{9.25mm}\right)}{2\pi f} \quad (7)$$

Finally, the position dependent losses are weighted with the time factor t_m for the calculation of the average losses during one beat cycle.

$$P_{avg} = f \cdot \left(\sum_{m=0}^{36} P_{sum,fw}(x_m) \cdot t_m + P_{sum,bw}(x_{37-m}) \cdot t_{37-m}\right) \quad (8)$$

Based on this tool chain, the drive is optimised by a combination of analytical and numerical computations to achieve accurate results in a minimum of computation time.

III. OPTIMIZATION METHODS

When comparing the 400 g of the human natural heart with the weight of the introduced drive, it is obvious that its weight has to be reduced. This can be achieved by optimizing the drive`s geometry and therefore reducing for example the height or the outer diameter of the drive. From the Lorentz force equation (1) it can be deduced that a drop of the induction $B_n(x)$, caused by a reduced permanent magnet volume, or a reduced active wire lengths l, results in lower producible forces. If the same forces $F_n(x)$ should be provided, the current supply of the coils $I_n(x)$ has to be increased, which increases the resulting losses as well. But in [6] it is stated that the electric losses in the drive have to be limited to 21 W in order to keep the rise of temperature in the human body below 1 °C. This statement has been proven by temperature measurements in the total artificial heart ReinHeart, which was developed at the RWTH Aachen University [7], during Mock Loop tests. For these reasons a weight reduction of the drive by an optimization of its geometry is possible. Although the allowable losses are 20 W, the drive of the artificial heart should be optimized in such a way that the required force is provided, while the resulting losses are in the range of 10 W and the weight is as low as possible. The reason for the lower loss limit lies in the peripheral components like the battery for example, which also should be light weighted and small sized. This approach will automatically reduce the dimensions of the drive as well.

A. Manual parameter variation

During the manual parameter variations a limited number of objective variables is selected to study their influence on the resulting losses and the weight of the drive. This is achieved by varying each parameter with a fixed step width. For example, the outer radius was decreased in steps of 1mm (Fig. 5). By evaluating the resulting weight vs. losses plots a hierarchic order is established, which indicates the best geometry parameters to be varied. In this paper the influence of the inner and outer radius as well as the thickness of the coils is presented and discussed. At the end the optimization algorithm has to find the best parameter combination for the optimum geometry of the drive while being within the allowed range of maximum losses.

In Fig. 5 the outer radius is decreased and the inner diameter is increased in steps of 1 mm. For the reduced outer radius the minimal weight in the diagram amounts to 495 g and resulting losses of 10.7 W. For the variation of the inner radius the minimal weight only amounts to 582 g and the losses accumulate to 9.7 W. In this case the achievable weight reduction is minimal. For this reason it is preferable to reduce the outer radius before increasing the inner radius.

In Fig. 6 the effect of the coil thickness is investigated. Therefore the outer radius is reduced for a coil thickness of 2 mm and a coil thickness of 3 mm. The average coil radius is identical for both arrangements, but the radial dimensions are symmetrically reduced for the thinner coil. This approach

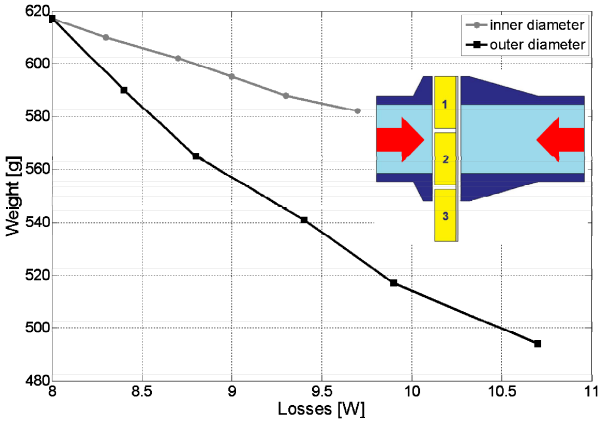

Fig. 5 Variation of inner and outer diameter.

increases the quotient of air in the air gap. When scaling the permanent magnets and the pole shoes in radial direction, this quotient is reduced again. Thus, a reduction of the drive's weight is achieved, because the material density of the copper wire (8.92 g/cm^3) is higher than for the NdFeB magnets (7.4 g/cm^3) and for the Vacoflux (8.12 g/cm^3) used for the pole shoes. Additionally, the axial height of the coils amounts about twice the magnets and pole shoes height, decreasing the weight further. On the other hand, the coil's resistant is increasing due to the reduced cross section of the coils, downgrading the drive's losses. This effect is partially compensated by the reduction of the leakage flux, concentrating the flux density in the air gap more effective. These complex correlations yield the intersection between the two curves in the range of 10.6 W losses and 500 g weight. When decreasing the outer radius even more, the losses are lower for a coil thickness of 2 mm.

B. Differential Evolution

DE is an evolutionary optimization algorithm, which is adapted for the optimization of the artificial drive, studied in this paper [8],[9]. In a first step the optimization parameters and their constraints are set. Then a population of random models, based on these parameters, is created. The quality of each model is determined by a predefined cost function:

$$cf = a \cdot 10^{\left(\frac{|losses - 10|}{10}\right)} + b \cdot 10^{\left(\frac{weight}{616}\right)} \quad (9)$$

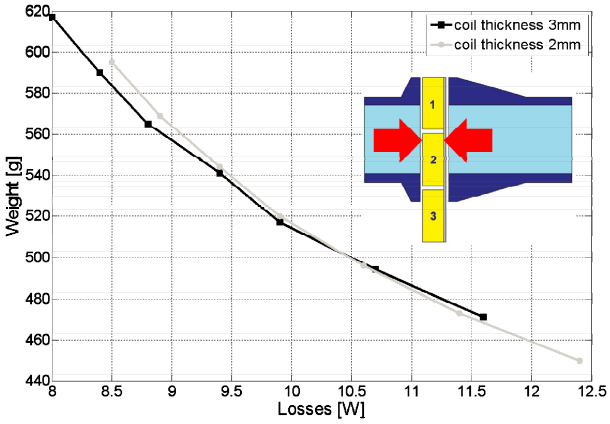

Fig. 6 Variation of coil thickness.

In order to give priority either to the losses or to the resulting weight during the optimization process the parameters a and b are initialized with a value between 0 and 1, while the sum of a and b equals to 1. For this reason the best model in theory has losses of 10 W, while its weight amounts to 0 g. Based on the best model of this population a new generation is created. After several iterations this process yields the optimum geometry of the drive without exceeding the allowed losses [10] when the algorithm is converging. In order to accelerate this process a cost function trigger was established. Before evaluating the cost function, the resulting losses for all models are determined. If they exceed the given limit, their values are multiplied with a factor of 10. As a result the cost function value is significantly increased.

The results of the DE algorithm are presented in Fig. 8. For all plots the x axis represents the number of iterations, while the label of the y axis is given in the title of each plot. The convergence of the DE algorithm is shown in plot b by the mean distance to the cost function of each model generation. In the first generation the means distance amount to a value greater than 10^5. After decreasing quickly it is nearly constant when reaching iteration number 28. After this iteration, there are only slight differences in the best models for the following generations. In this plot the cost function of the best model are not shown for the first 11 iterations in order to be able to follow the variations at the middle and the end of the algorithm. By analyzing plot c and d, the operation principle of the DE algorithm is illustrated. In the applied cost function the priority is given to the losses. At the beginning the losses are exceeding the given limit. Due to the cost function trigger, these models are penalized, what yields a high cost function value. As a result the weight is reduced by changing the drive´s geometry as indicated in the plot e - i. This yields a fast reduction of the mean cost function in plot b at the beginning. After the 12 th iteration the losses fall below the limit of 10 W. By reducing the weight further the losses are rising again up to its global maximum of 9.99 W for the final model. Starting with iteration number 20 the losses are constant, but the weight is reduced further to its final value of 460 g.

IV. RESULTS

The final geometry parameters and the resulting weight and losses are collected in Table 1 for the two optimization methods and the prototype. During parameter variations and DE optimization the resulting losses amount to 9.94 W and 9.99 W respectively, what is close to the desired loss limit of 10 W. When compared to the prototype the losses are increased by 2 W. The higher loss limit enabled a weight reduction of the drive by 99 g for parameter variations and by 156 g for DE. This result is caused by the differences in the geometries, obtained by the two methods. While the inner radius (8 mm) and the outer radius (38.5 mm and 38.45 mm) are nearly identical, the maximum height of the static drive part is lower for the DE algorithm.

TABLE I
COMPARISON OF PROTOTYPE AND OPTIMIZED GEOMETRY

Paramerter	Prototype	Variation Calculations	Differential Evolution
Weight	616 g	517 g	460 g
Losses	8 W	9.94 W	9.99 W
Inner radius	7 mm	8 mm	8 mm
Outer radius	42.5 mm	38.5 mm	38.45 mm
Height max.	16.5 mm	16.5 mm	15.6 mm

This and further differences are shown in Fig. 7, which visually compares the drive geometries from the top to the bottom of the prototype (a), parameter variations (b) and DE algorithm (c). When comparing the axial dimensions of the magnets and the pole shoes, the magnet height is increased while the pole shoe height is decreased for the model c. Due to the lower material density of the magnets and the reduced height of the static part, the weight is declining for this drive when compared to drive b. In c the average radius and the thickness of the coils is reduced as well. On one hand the electric losses are increased due to reduction of the active wire length l , on the other hand the balance between the induction $B_n(x)$ generated by the inner and outer permanent magnets is changed, when compared to model b. For these reasons a higher weight reduction was reached for the DE algorithm while the resulting losses were close to the ones, occurring in the model, obtained by parameter variations.

V. CONCLUSIONS

This paper reports on the optimization of the geometry of a drive, which operates a pulsatile artificial heart. After introducing the prototype of the drive and its constraints for implantation, the two optimization approaches, parameter variation and DE are explained. Both rely on a calculation chain, which is a combination of FEM simulation to determine the distribution of the magnetic induction and analytical equations, which are applied to calculate the resulting weight and the losses of the drive. The new drive geometries, gained by the two optimization approaches are close to the loss limit of 10 W. When comparing the resulting weights, the reduction is higher for the DE approach. During parameter variation the

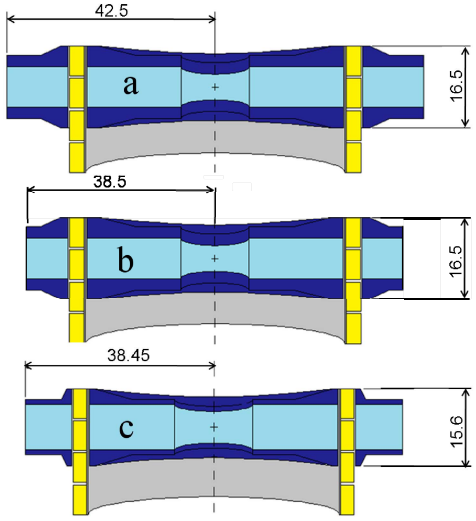

Fig. 7 Visualization of optimization results.

geometry parameters are varied with a fixed step width. The resulting weight vs. loss plots show clearly the sensitivity of the applied parameters. By this way a hierarchic order is established, which indicates the best parameter to vary for a given loss limit. The disadvantage of this approach is that only one parameter can be actively changed, but the investigated geometry parameter are all interdependent. During the DE optimization process the computer model are created by randomly chosen parameters and therefore take these dependencies into account. When the algorithm is converging the best possible results according to the cost function is obtained. On the negative side the effect of each parameter is not traceable, because they are initialized with randomly chosen values. Further, the amount of required computer models is much higher, when compared to the parameter variation, due to the working principle of DE. As the probability of non-convergence is rising with the increase of parameters, a combination of both optimization approaches is advisable. After gaining the knowledge of the sensitivity of some geometry parameters, the amount of parameters can be reduced for the next DE optimization step. Additionally, the required number of models and therefore the computation time is reduced as well. DE proposed a coil thickness of 2.7 mm. As the producible coil thickness depends on the available copper wire, an adjustment of the DE results due to manufacturing is necessary.

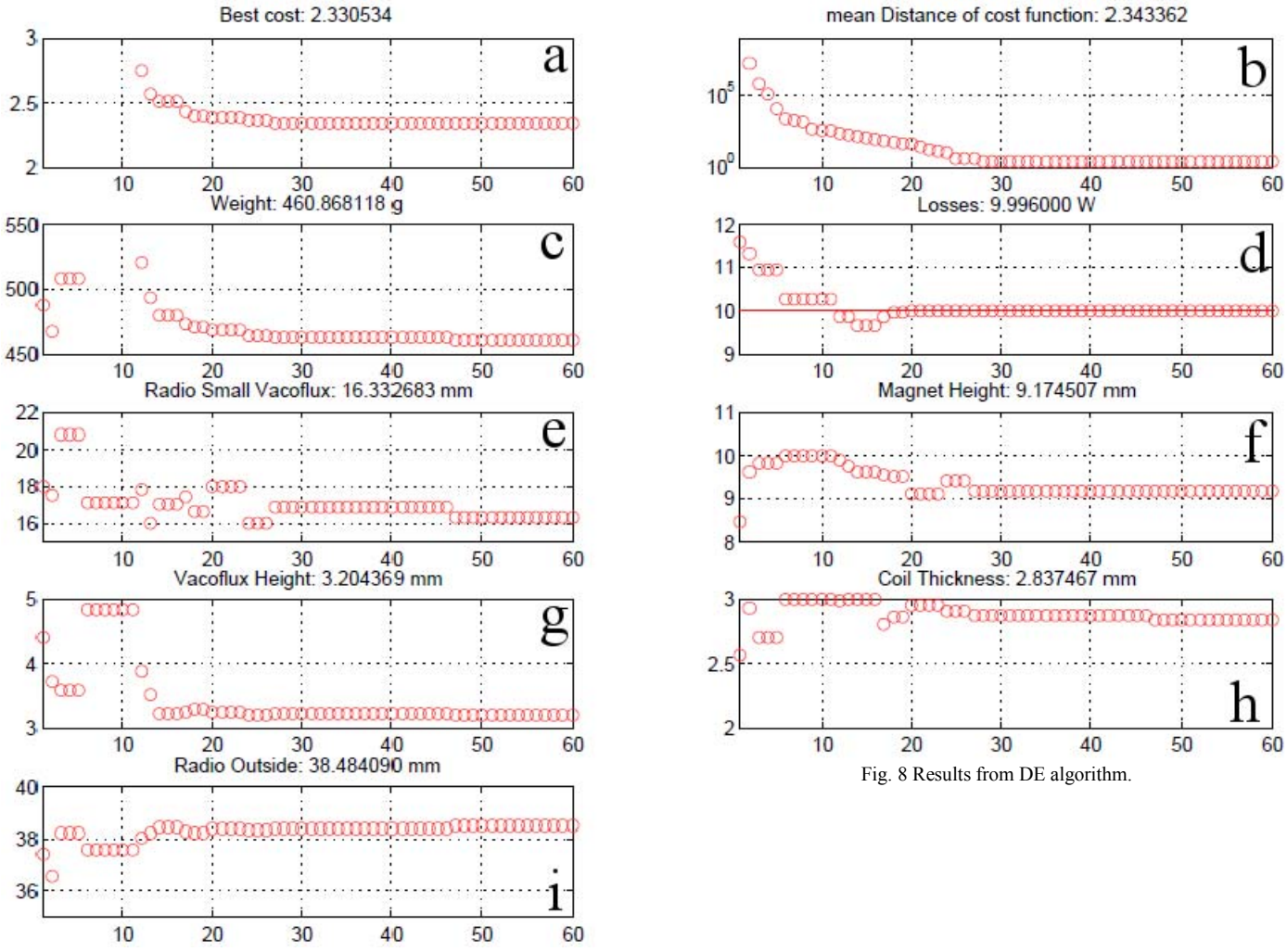

Fig. 8 Results from DE algorithm.

REFERENCES

[1] Abstracts from the 14th Congress of the International Society for Rotary Blood Pumps. Artif. Organs, 2006, 30(11): A27.

[2] M. Lessmann, T. Finocchiaro, U. Steinseifer, T. Schmitz-Rode and K. Hameyer, "Concepts and designs of life support systems." IET Science, Measurement & Technology 2008, 2(6): 499-505.

[3] www.vacuumschmelze.de, accessed February 2010

[4] A. Pohlmann, M. Leßmann, T. Finocchiaro, A. Fritschi, T. Schmitz-Rode, and K. Hameyer, "Drive optimisation of a pulsatile Total Artificial Heart", in: the XXI symposium electromagnetic phenomena in nonlinear circuits, EPNC 2010, pages 65-66, 2010.

[5] www.iem.rwth-aachen.de, accessed May 2010

[6] M. Yamaguchi, T. Yano, M. Karita, Y. Yamamoto, S. Yamada and H. Yamada, "Performance Test of a Linear Pulse Motor-Driven Artificial Heart", IEEE Translation Journal in Japan, Vol. 8, No. 2, February 1993.

[7] A. Pohlmann, M. Leßmann, T. Finocchiaro, T. Schmitz-Rode, and K. Hameyer, "Numerical computation can safe life: FEM simulations for the development of artificial hearts", The 14th International Conference on Electromagnetic Field Computation, CEFC, Chicago, USA, May 2010

[8] K. V. Price, R. M. Storn and J. A. Lampinen, "Differential Evolution - A Practical Approach to Global Optimization", 1st ed., Springer, 2005.

[9] U. K. Chakraborty, "Advances in Differential Evolution", Springer, 2008.

[10] Hameyer, K., Belmans, R.: Numerical modelling and design of electrical machines and drives, Computational Mechanics Publications, WIT Press, Southampton 1999.